

# Thermal annealing of femtosecond laser written structures in silica glass

Jonathan J. Witcher,<sup>1</sup> Wilbur J. Reichman,<sup>1</sup> Luke B. Fletcher,<sup>1</sup> Neil W. Troy,<sup>1</sup> and Denise M. Krol<sup>2,\*</sup>

<sup>1</sup>Department of Applied Science, University of California Davis, Davis, California 95616, USA

<sup>2</sup>Department of Chemical Engineering & Materials Science, University of California Davis, Davis, California 95616, USA

\*dmkrol@ucdavis.edu

**Abstract:** We have investigated the thermal stability of femtosecond laser modification inside fused silica. Raman and FL spectroscopy show that fs-laser induced non-bridging oxygen hole center (NBOHC) defects completely disappear at 300 °C, whereas changes in Si-O ring structures only anneal out after heat treatment at 800-900 °C. After annealing at 900 °C optical waveguides written inside the glass had completely disappeared whereas more significant damage induced in the glass remained. The results are related to different types of bond rearrangements in the glass network.

© 2013 Optical Society of America

**OCIS codes:** (320.2250) Femtosecond phenomena; (220.4000) Microstructure fabrication; (230.7370) Waveguides; (160.2750) Glass and other amorphous materials.

---

## References and links

1. K. M. Davis, K. Miura, N. Sugimoto, and K. Hirao, "Writing waveguides in glass with a femtosecond laser," *Opt. Lett.* **21**(21), 1729–1731 (1996).
2. E. N. Glezer, M. Milosavljevic, L. Huang, R. J. Finlay, T. H. Her, J. P. Callan, and E. Mazur, "Three-dimensional optical storage inside transparent materials," *Opt. Lett.* **21**(24), 2023–2025 (1996).
3. K. Itoh, W. Watanabe, S. Nolte, and C. Schaffer, "Ultrafast processes for bulk modification of transparent materials," *MRS Bull.* **31**(08), 620–625 (2006).
4. K. Miura, J. Qiu, H. Inouye, T. Mitsuyu, and K. Hirao, "Photowritten optical waveguides in various glasses with ultrashort pulse laser," *Appl. Phys. Lett.* **71**(23), 3329–3331 (1997).
5. W. Watanabe, T. Asano, K. Yamada, K. Itoh, and J. Nishii, "Wavelength division with three-dimensional couplers fabricated by filamentation of femtosecond laser pulses," *Opt. Lett.* **28**(24), 2491–2493 (2003).
6. G. D. Marshall, M. Ams, and M. J. Withford, "Direct laser written waveguide-Bragg gratings in bulk fused silica," *Opt. Lett.* **31**(18), 2690–2691 (2006).
7. W. Watanabe, D. Kuroda, K. Itoh, and J. Nishii, "Fabrication of Fresnel zone plate embedded in silica glass by femtosecond laser pulses," *Opt. Express* **10**(19), 978–983 (2002).
8. T. Pertsch, U. Peschel, F. Lederer, J. Burghoff, M. Will, S. Nolte, and A. Tünnermann, "Discrete diffraction in two-dimensional arrays of coupled waveguides in silica," *Opt. Lett.* **29**(5), 468–470 (2004).
9. A. M. Kowalevich, V. Sharma, E. P. Ippen, J. G. Fujimoto, and K. Minoshima, "Three-dimensional photonic devices fabricated in glass by use of a femtosecond laser oscillator," *Opt. Lett.* **30**(9), 1060–1062 (2005).
10. D. Homoelle, S. Wielandy, A. L. Gaeta, N. F. Borrelli, and C. Smith, "Infrared photosensitivity in silica glasses exposed to femtosecond laser pulses," *Opt. Lett.* **24**(18), 1311–1313 (1999).
11. J. W. Chan, T. Huser, S. Risbud, and D. M. Krol, "Structural changes in fused silica after exposure to focused femtosecond laser pulses," *Opt. Lett.* **26**(21), 1726–1728 (2001).
12. J. W. Chan, T. R. Huser, S. H. Risbud, and D. M. Krol, "Modification of the fused silica glass network associated with waveguide fabrication using femtosecond laser pulses," *Appl. Phys., A Mater. Sci. Process.* **76**(3), 367–372 (2003).
13. D. M. Krol, "Femtosecond laser modification of glass," *J. Non-Cryst. Solids* **354**(2-9), 416–424 (2008).
14. Y. Bellouard, E. Barthel, A. A. Said, M. Dugan, and P. Bado, "Scanning thermal microscopy and Raman analysis of bulk fused silica exposed to low-energy femtosecond laser pulses," *Opt. Express* **16**(24), 19520–19534 (2008).
15. M. Sakakura, M. Terazima, Y. Shimotsuma, K. Miura, and K. Hirao, "Thermal and shock induced modification inside a silica glass by focused femtosecond laser pulse," *J. Appl. Phys.* **109**(2), 023503 (2011).
16. E. Bricchi and P. G. Kazansky, "Extraordinary stability of anisotropic femtosecond direct-written structures embedded in silica glass," *Appl. Phys. Lett.* **88**(11), 111119 (2006).

17. V. R. Bhardwaj, P. B. Corkum, D. M. Rayner, C. Hnatovsky, E. Simova, and R. S. Taylor, "Stress in femtosecond-laser-written waveguides in fused silica," *Opt. Lett.* **29**(12), 1312–1314 (2004).
  18. W. J. Reichman, D. M. Krol, L. Shah, F. Yoshino, A. Arai, S. M. Eaton, and P. R. Herman, "A spectroscopic comparison of femtosecond-laser-modified fused silica using kilohertz and megahertz laser systems," *J. Appl. Phys.* **99**(12), 123112 (2006).
  19. D. M. Krol, K. B. Lyons, S. A. Brawer, and C. R. Kurkjian, "High-temperature light scattering and the glass transition in vitreous silica," *Phys. Rev. B Condens. Matter* **33**(6), 4196–4202 (1986).
  20. R. Brüning and D. Cottrell, "X-ray and neutron scattering observations of structural relaxation of vitreous silica," *J. Non-Cryst. Solids* **325**(1-3), 6–15 (2003).
- 

## 1. Introduction

The use of femtosecond lasers to modify the bulk of transparent materials has proven to be an important method for the fabrication and integration of optical components, such as waveguides, splitters, Bragg gratings, and amplifiers [1–10]. Significant work has been done on the creation and characterization of waveguides inside glass as well as microscopic characterization of fs-laser modification. In fused silica, fs-laser written waveguides are accompanied by structural changes in the glass, which include non-bridging oxygen hole center (NBOHC) fluorescence defects and changes in the glass network structure (three-membered Si-O ring concentration) [11–15].

The long-term stability of fs-laser modification is extremely important for any practical use of fs-laser written devices. For example, any optical circuit created via fs-laser waveguide writing will need to have stable operation over the lifetime of the device at standard operating temperatures. Previous work has shown that the fluorescence signal from non-bridging oxygen hole center (NBOHC) defects, which are created in the fs-laser modification process, decreases under low power 488 nm continuous laser exposure [12]. This illustrates the relatively low stability of the NBOHC defects. Even when the NBOHC defects were removed, the waveguide structures remained. A few groups have reported the effects of thermal annealing on the refractive index and loss of fs-laser written structures in fused silica [16,17] and observed complete erasure of the structures around 1100 °C, but these studies did not investigate how such changes in optical properties were correlated with structural changes at the atomic-scale level. Studying the thermal annealing behavior, both microscopically and macroscopically, is important to gain a greater understanding of the stability of fs-laser written structures.

In this paper we systematically study the effects of thermal annealing on fs-laser modification in fused silica. The effects of varying annealing temperatures as well as annealing times are investigated with respect to visible characteristics, guiding behavior and microscopic changes in glass structure as measured using fluorescence and Raman spectroscopy. "Rough" modification that results in poor quality waveguides remain visibly unchanged at annealing temperatures of up to 900 °C even after localized defects and glass-network structure are returned to unmodified levels due to the annealing. "Good" quality waveguides that exhibit guiding at 660 nm can be completely annealed out at 900 °C, a temperature that is well below the glass transition temperature of fused silica (~1300 °C). The results of our study point to a significant difference between fs-laser written structures that result in good quality (smooth) waveguides and those resulting in poor quality (rough) waveguides.

## 2. Experimental setup and procedures

For fs-laser writing two different amplified Ti-sapphire laser systems with slightly different specifications and writing procedures, as summarized in Table 1, were used. Both laser systems, Spitfire and Hurricane (both from Spectra Physics), were operated at 800 nm with a repetition rate of 1 KHz. For the experiments with the Spitfire laser a transverse writing geometry was used, whereas in the case of the Hurricane laser a longitudinal writing geometry was employed.

Standard grade fused silica samples (Corning 7980) were used in all experiments. For the experiments with the Spitfire laser 4 samples (each  $19.5 \times 19.5 \times 5 \text{ mm}^3$ ) were used. In each sample an identical set of lines of varying pulse energy (see Table 1) was written. With the Hurricane laser 3 samples were prepared (each  $19.5 \times 19.5 \times 1.7 \text{ mm}^3$ ), each also with an identical set of lines of varying pulse energies (see Table 1). Throughout this paper fs-laser written lines will be identified by the set label (A and B in Table 1) and the pulse fluence, i.e. line B-40 is a line written with the Spitfire laser system at a pulse fluence of  $40 \text{ J/cm}^2$ .

**Table 1. Fs-laser Writing Conditions**

	<b>Set A Hurricane laser system</b>	<b>Set B Spitfire laser system</b>
pulse energy	0.9, 1.3, 1.7, 2.6 $\mu\text{J}$	0.5, 0.7, 3.4, 13.4 $\mu\text{J}$
pulse duration	150 fs*	140 fs*
focusing objective	10x / 0.25NA	50x / 0.55NA
pulse fluence	11, 16, 21, 32 $\text{J/cm}^2$	28, 40, 200, 800 $\text{J/cm}^2$
sample scan speed	50 $\mu\text{m/s}$	40 $\mu\text{m/s}$
writing geometry	longitudinal	transverse
annealing temperatures	300, 600, 800, 900 $^\circ\text{C}$	100, 300, 600, 900 $^\circ\text{C}$
annealing times	5, 10, 60, 600 mins	5, 10, 60, 600 mins

\*pulse duration measured with a single-shot autocorrelator

After the fs-laser writing experiments the lines were analyzed by white light microscopy as well as confocal Raman and fluorescence (FL) microscopy. Each sample was subsequently placed in a furnace for a prescribed time and temperature and then removed. A different sample was used for each annealing temperature chosen. After cooling back to room temperature the sample was again analyzed. This process was repeated over multiple annealing times. To avoid the affects of photobleaching [12] during the Raman and FL experiments, spectra were collected at a different position within the fs-laser written line after each annealing treatment. No two fluorescence spectra were collected from the same point in the modified (or unmodified) sample. In total 5 annealing temperatures and 4 annealing times were investigated for each of the different waveguide writing energies (cf. Table 1). The annealing time refers to the total time at temperature of the sample. For example, in the  $100 \text{ }^\circ\text{C}$  sample the furnace is first brought up to  $100 \text{ }^\circ\text{C}$  until the temperature stabilizes at which point the sample is placed in the furnace. After 5 minutes it is removed and allowed to cool to room temperature and then white light microscopy and Raman/FL measurements are performed on this “5 min annealed” sample. After these measurements the sample is placed back into the  $100 \text{ }^\circ\text{C}$  furnace for an additional 5 minutes at which time it is removed, cooled to room temp and again investigated, now as the “10 min annealed” sample.

White light images of the modified areas were collected using a 50x (0.55 NA) objective and a CMOS camera. A 10x (0.25 NA) objective was used to focus 660 nm laser light into the input waveguide facet, and a 20x (0.40 NA) objective was focused at the output facet in order to characterize the guiding properties. Mode profiles of the transmitted 660 nm laser light were obtained by imaging the near-field intensity at the output facet of the waveguide using a Canon Rebel T1i CMOS camera.

Confocal Raman and FL microscopy was performed on the fs-laser induced modifications using an adjustable power 473 nm cw laser. The 473 nm excitation beam was directed through a high NA focusing objective using a 50/50 broadband dichroic beam splitter and focused into the glass sample. Backscatter signals produced by the 473 nm laser excitation were collected by the same objective and directed through the 50/50 beam splitter. A pinhole with a 50  $\mu\text{m}$  diameter was used to ensure Raman signals were only collected from the focal volume of the objective. A spectrometer (Oriel MS257) in conjunction with a CCD camera (TEC-CCD

Princeton Instruments) was used to collect spectral signals that passed through the pinhole setup. The spectrometer was used with a 1200 grooves/mm grating centered at 500 nm to collect Raman signals, and a 600 grooves/mm grating centered at 620 nm to collect fluorescence signals.

### 3. Results and discussion

#### 3.1 Optical microscopy

Figure 1 shows white light microscopy images of fs-laser written lines, sets A and B, in fused silica before any annealing of the sample. Of all the lines that were fabricated only lines from set A written with fluences of 11, 16 and 21 J/cm<sup>2</sup> exhibited good guiding. In the remainder of this paper we will refer to these lines as ‘waveguides’; all other lines will be referred to as ‘damage lines’.

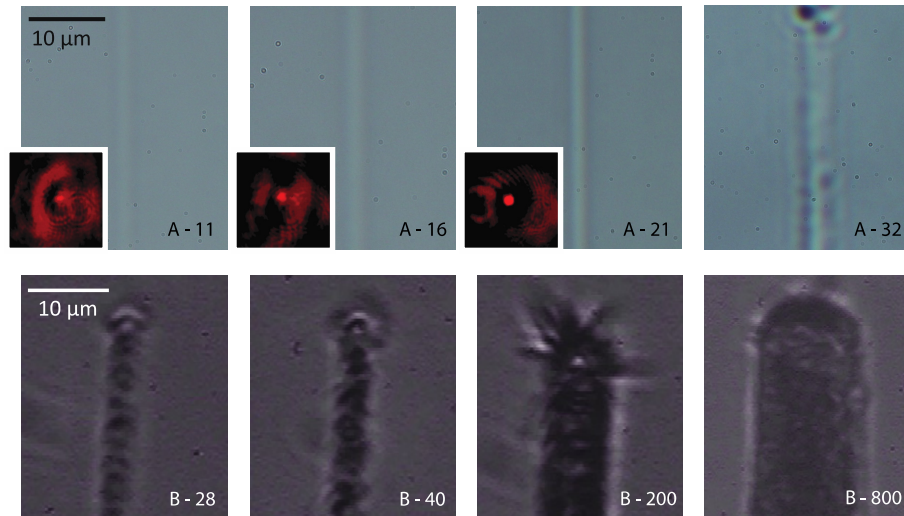


Fig. 1. White light microscopy images of lines written in fused silica before annealing. Lines written in samples A11, A16 and A21 exhibited guiding of 660 nm light as illustrated by the near-field output profile shown in the inset. The labels refer to the fs laser writing conditions. The letter refers to the fs-laser used and the number to the laser pulse fluence (see also Table 1).

After annealing experiments at 300 °C for 10 hours none of the lines showed any visible change in white light microscopy. Figure 2 shows the annealing behavior at 600 and 900 °C for several of the lines. At these temperatures the damage lines still remain unchanged, but the waveguides become fainter at 600 °C and 800 °C and have disappeared completely at 900 °C. This observation is further supported by the fact that at 800 °C the lines no longer guide when trying to couple light from a He-Ne laser.

#### 3.2 Confocal fluorescence and Raman microscopy

In order to obtain further insight into the annealing behavior of the fs laser written waveguide and damage lines, we have performed confocal fluorescence and Raman microscopy experiments. Figure 3 shows the FL spectra of waveguides (Fig. 3a) and damage lines (Fig. 3b) before any annealing takes place. These spectra are in agreement with what we have observed in earlier studies on fs-laser modification in fused silica: when using writing conditions that result in good waveguides the modified material exhibits a ~540 nm fluorescence, assigned to self trapped exciton ( $E_s$ ) defects from very small silicon nano-

clusters [18]. The rough modification, produced when using higher laser intensities, is characterized by a red fluorescence peak centered at 650 nm, due to NBOHC defects.

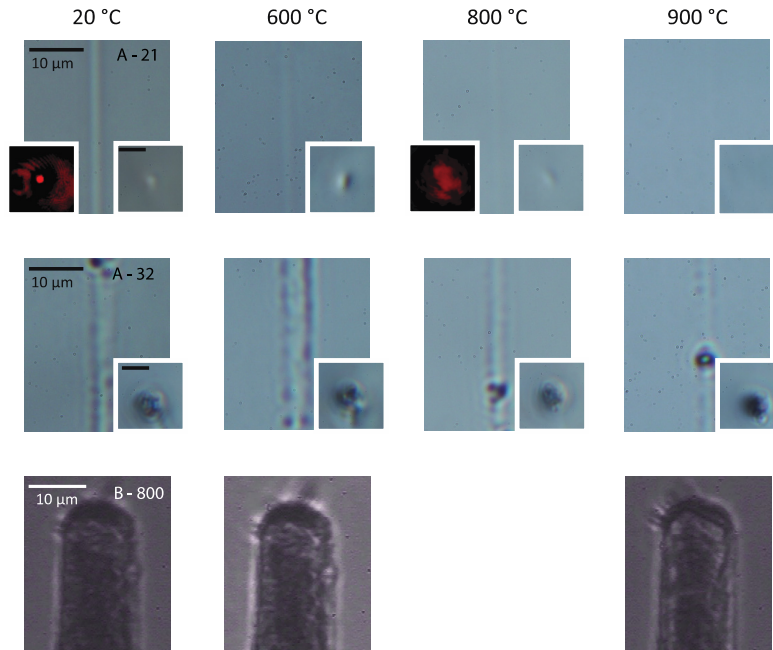


Fig. 2. White light microscopy images of lines written in fused silica before annealing (left column), and after annealing for 10 hours at 600, 800 and 900 °C (column 2, 3 and 4). Line labels are explained in the text. The inset on the right of each image shows the cross-sectional view for white light microscopy. The inset on the left in the top row shows the near-field profile for 660 nm laser light.

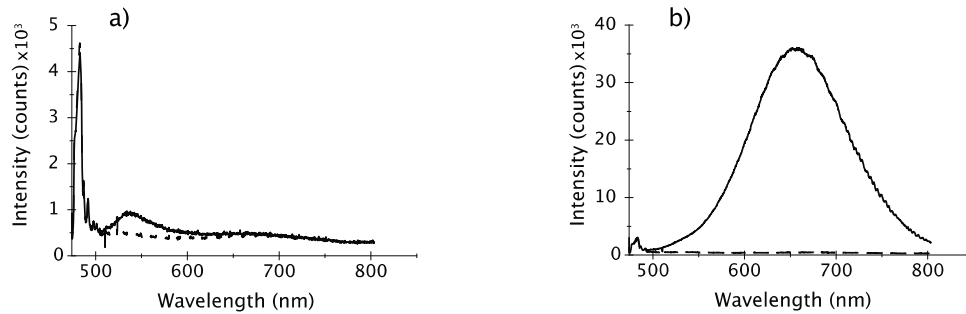


Fig. 3. Fluorescence spectra of modified (solid curves) and unmodified (dashed curves) fused silica; the glass was modified with a pulse fluence of a) 21 J/cm<sup>2</sup> and b) 32 J/cm<sup>2</sup>.

Figures 4 and 5 summarize the annealing behavior of the NBOHC defects as monitored through the fluorescence at 650 nm. Figure 4 displays the results for lines modified with different fs-laser pulse fluences after annealing for 10 hrs at different temperatures, whereas Fig. 5 shows the time dependence of the annealing behavior for two of the lines. Qualitatively similar results are observed for the other lines.

As expected, the initial defect concentration before annealing (data points at 20 °C) increases with increasing fs-laser pulse fluence. No NBOHC fluorescence is seen in the unmodified sample because the defects are not significantly present before fs-laser modification.

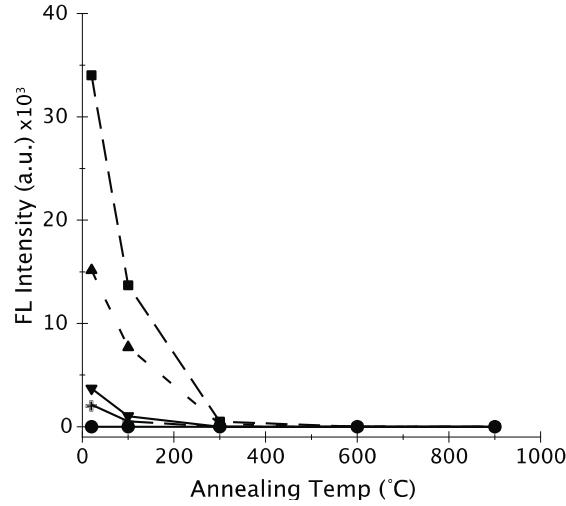


Fig. 4. Area under 650 nm NBOHC FL peak for fs-laser written lines annealed for 10 hours as a function of annealing temperature. Data are shown for lines written with different pulse fluences: ■ – 800 J/cm<sup>2</sup>; ▲ – 200 J/cm<sup>2</sup>; ▼ – 40 J/cm<sup>2</sup>; + – 28 J/cm<sup>2</sup> and ● – unmodified sample.

The results in Fig. 4 show that for a 10 hour annealing time the defects completely anneal out at a temperature as low as 300 °C. Note that at this temperature there is no change in morphology in any of the lines when viewed with white light microscopy. The graphs in Fig. 5 show that the NBOHC defects disappear faster with increasing annealing temperature. At 100 °C there are still some defects presents after 10 hours of annealing, but at 300 °C and above the defects are completely gone after 10 hours or less. When annealing at 600 °C the NBOHC defects from the damage lines completely disappear after only 5 min annealing time. The 530 nm fluorescence that accompanies fs-written waveguides (Fig. 3a) also completely anneals out after 10 hours or less at 300 °C.

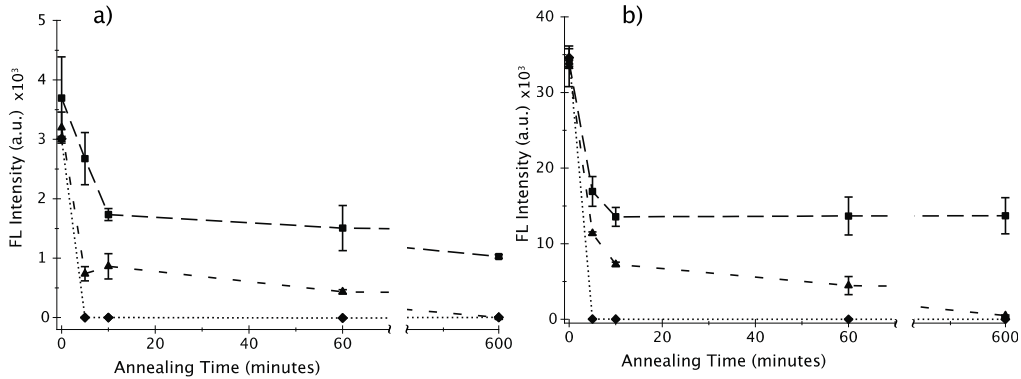


Fig. 5. Area under 650 nm NBOHC peak for lines written with a fs laser pulse fluence of a) 40 J/cm<sup>2</sup> and b) 800 J/cm<sup>2</sup> as a function of annealing time at different annealing temperatures: ■ – 100 °C; ▲ – 300 °C; ◆ – 600 °C.

Overall the FL data do not correlate with the annealing behavior that is seen with white light microscopy. The FL signals anneal out at much lower temperatures than the features

seen under the microscope, indicating that localized defects such as NBOHC are not the main cause of the structural changes associated with waveguides or damage lines.

In previous studies [11,12] we have shown that fs-laser modification is accompanied by changes in the Raman spectrum of the glass, in particular in the relative intensity of the peak at  $605\text{ cm}^{-1}$ , which is due to 3-membered Si-O rings. Figure 6 shows the Raman spectra of the unmodified fused silica sample and of two of the fs-laser written lines, one written with the Spitfire and one with the Hurricane laser system. The line written at a fluence of  $32\text{ J/cm}^2$  using the longitudinal writing geometry results in a larger  $605\text{ cm}^{-1}$  peak than the line written at  $40\text{ J/cm}^2$  in the transverse geometry. This is probably due to the fact that in the longitudinal writing geometry the total exposure (number of pulses per unit volume) is larger.

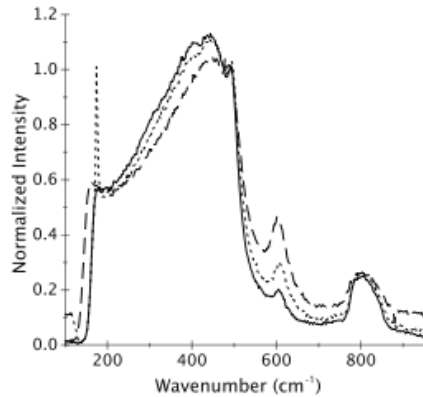


Fig. 6. Raman spectra of fs-laser written lines in fused silica; line A-32 (large-dashed curve), B-40 (small-dashed curve) and the unmodified sample (solid curve).

Figure 7 shows the  $605\text{ cm}^{-1}/800\text{ cm}^{-1}$  Raman ratio (relative concentration of 3-membered Si-O rings) for lines written with different pulse fluences after annealing for 10 hours at different temperatures. First of all, the results show that within a certain set (A or B) the initial increase in Raman ratio (data at  $20\text{ }^{\circ}\text{C}$ ) is larger for lines written with higher pulse fluences, similar to what we observed in earlier studies [11–13].

The increase in relative 3-membered Si-O ring concentration in the fs-laser written lines is significantly more resistant to thermal annealing than the NBOHC defects. Within the experimental error the relative concentration of 3-membered rings does not show any significant changes below  $600\text{ }^{\circ}\text{C}$ . An accurate determination of the Raman ratio at  $T < 600\text{ }^{\circ}\text{C}$  is somewhat hampered by the changing intensity in the (tail of the) FL spectral signal which changes in this temperature range. The data also show that most of the Raman changes are annealed out above  $600\text{ }^{\circ}\text{C}$ . In order to find out what happens above  $600\text{ }^{\circ}\text{C}$  we have performed a more detailed Raman analysis on samples annealed at  $800$  and  $900\text{ }^{\circ}\text{C}$ , temperatures where the white light microscopy results show the most significant changes. The results in Fig. 7 show that after annealing for 10 hours at  $800$  or  $900\text{ }^{\circ}\text{C}$  the Raman ratio returns, within experimental error, to the value of the unmodified glass. This occurs for the smooth as well as the rough lines. In the case of the smooth lines (Fig. 2, top row and Fig. 7, bottom left) the Raman results are in agreement with the fact that the modification has completely disappeared after annealing at  $900\text{ }^{\circ}\text{C}$ . However, in the case of the rough lines (Fig. 2, bottom two rows and Fig. 7, bottom row) the damage lines are still clearly visible after the  $900\text{ }^{\circ}\text{C}$  anneal while the Raman data are representative of the structure of the unmodified glass. We think that this is related to the fact that in the case of damage lines the structural changes are accompanied by void formation. Upon annealing at  $900\text{ }^{\circ}\text{C}$  the glass structure in the damage regions relaxes back to that of the unmodified glass in terms of ring statistics but without closing the voids. The structural changes that are necessary to eliminate the voids



probably would require heating to temperatures close to the glass transition temperature of fused silica ( $T_g \approx 1100 \text{ }^\circ\text{C}$ ).

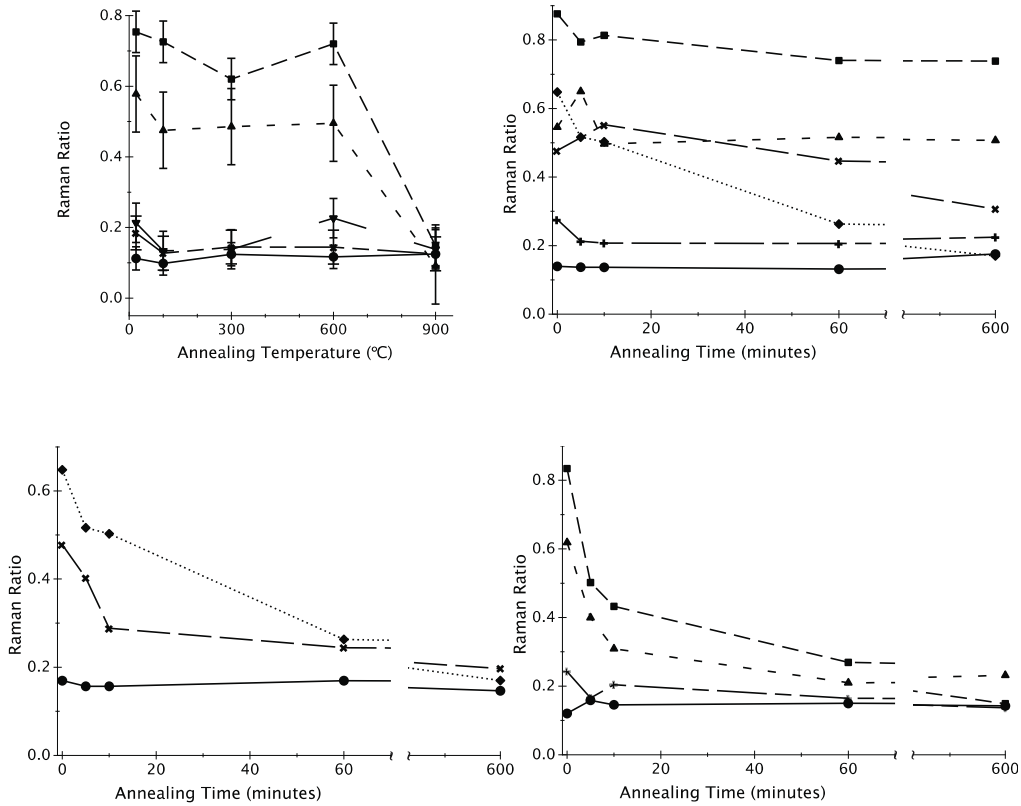
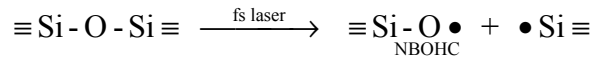


Fig. 7.  $605 \text{ cm}^{-1}/800 \text{ cm}^{-1}$  Raman intensity ratio for fs-laser written lines. Raman intensity after annealing at different temperatures for 10 hours (top left). Raman intensity as a function of annealing time at  $600 \text{ }^\circ\text{C}$  (top right),  $800 \text{ }^\circ\text{C}$  (bottom left), and  $900 \text{ }^\circ\text{C}$  (bottom right). Data are shown for different lines: ■ B-800; ▲ B-200; ◆ A-32; + B-28; × A-21 and ● – unmodified sample.

The large differences in annealing temperature for NBOHC defects and Si-O ring structures are related to the fact that different types of structural rearrangements are involved. NBOHC defects can be produced by breaking a single bond in the 3D silica network via the following reaction:



It is expected that the activation energy for repairing such a single broken bond, and thus removing the defect, is relatively low, in agreement with the fact that NBOHC defects disappear at a low annealing temperature of  $300 \text{ }^\circ\text{C}$  or when the sample is exposed to cw visible laser light [12]. The structural rearrangements that are needed to change the ring statistics in the silica network require more complex bond changes involving multiple atoms and changes in the medium range order of the glass network. Such changes require much higher temperatures of  $800\text{-}900 \text{ }^\circ\text{C}$ , although even these temperatures are well below  $T_g$ . These results are in agreement with earlier investigations on sub- $T_g$  relaxations in fused silica samples with high fictive temperature, which also showed changes in ring statistics below  $T_g$  [19]. Structural relaxation and changes in medium range order at temperatures as low as  $800\text{-}900 \text{ }^\circ\text{C}$  have also been observed in x-ray and neutron scattering experiments [20].



In conclusion, we have investigated the effects of thermal annealing on femtosecond laser modification inside fused silica. Raman and FL spectroscopy show that fs-laser induced NBOHC defects completely anneal out at 300 °C, whereas changes in Si-O ring structure only anneal out after heat treatment at 800-900 °C. At 900 °C optical waveguides written inside the glass were completely annealed but more significant damage induced in the glass remained after annealing at that temperature.

### **Acknowledgments**

The authors thank C.R. de Kok of Utrecht University, the Netherlands, for assistance with the waveguide writing experiments on the Hurricane laser system. The authors acknowledge financial support through NSF Grant No. NSF-DMR 0801786.